

# Improvement of Scattering Model Decomposition by ESPRIT-based Pol-InSAR

# Hitoshi Onoda<sup>1</sup>, Masahiro Yamazaki<sup>1</sup>, Hiroyoshi Yamada<sup>2</sup> Yoshio Yamaguchi<sup>2</sup>

<sup>1</sup> Graduate School of Science & Technology, Niigata University

Ikarashi 2-8050, Niigata-shi, 950-2181 Japan, {onoda,masahiro}@wave.ie.niigata-u.ac.jp

<sup>2</sup> Faculty of Engineering, Niigata University

Ikarashi 2-8050, Niigata-shi, 950-2181 Japan, {yamada,yamaguchi}@ie.niigata-u.ac.jp

## 1. Introduction

Observation of the global environment by microwave remote sensing technology has been attracting attention recently. Image classification is one of the important applications in POLSAR (Polarimetric SAR) image analysis. Various techniques are proposed. The scattering model decomposition [1] is one of the powerful techniques among them. This technique decomposes a covariance matrix derived by the POLSAR image data into three fundamental covariance matrices corresponding to single, double-bounce, and volume scattering component. However, when we apply the scattering model decomposition [1], we encounter problem that power of several components in some area becomes negative. This is caused by the assumptions used in the decomposition technique [1]; 1) assumption of the volume scattering matrices, and 2) one of the elements in the single or double-bounce scattering component is assumed to be known. Yamaguchi *et. al.* have proposed a modified technique which is referred as a conventional technique in the followings referred [2]. In this technique, the covariance matrix of the volume scattering is extended to three types. We can estimate a suitable matrix for decomposition among them. However, various types of volume scattering would exist in actual dataset. In addition, the assumption 2 is still required for this decomposition. The problem of the negative power components is improved by this technique. However there still remain several negative power areas. For the POLSAR image analysis, we only have three observables (HH, HV and VV data) so that further modification would be difficult.

In this paper, we propose a modified model decomposition algorithm for Pol-InSAR (Polarimetric and Interferometric SAR) images for forest area. For the Pol-InSAR image analysis, additional images in different orbit are available. As in [5], the volume scattering component in each image area can be directly estimated for the dataset. Main cause of negative components would be selection of the inadequate covariance matrix. Therefore, this cause can be removed by the proposed technique with Pol-InSAR analysis. In addition, more realistic assumptions for the single and double-bounce component decomposition are considered here to obtain further accuracy improvements. Experimental results for forest analysis by the proposed and conventional technique [2] is presented to show availability of the proposed technique.

## 2. Estimation of Optimal Volume Scattering Component with Pol-InSAR Dataset

For forest region, the covariance matrix of volume scattering component depends on distribution of tree trunks and branches. Since there are independent observables in POLSAR image analysis, direct estimation of the matrix is impossible. In [2], it is extended to select most suitable one among three types of distributions. Figure 1 shows the possible PDF (probability density function) of tree trunks and branches in the method [2], [3], [5]. Most optimal covariance matrix for the volume scattering,  $C_v$ , can be estimated among these PDF candidates.

Since pair of images can be available in Pol-InSAR analysis, therefore further extension can be realized for Pol-InSAR images analysis. We have proposed the ESPRIT-based Pol-InSAR technique

for forest tree height estimation of Pol-SAR data [4]. Estimation accuracy of the tree height can be improved by volume scattering component removal preprocessings [3], [5]. This preprocessing is based on the concept that two discrete scattering corresponding to the ground and canopy top will remain by removing volume scattering components with optimal distribution. By using this concept, we can estimate most suitable volume scattering matrix among more than three candidates. Therefore more precise estimation can be realized than that by the conventional technique [2]. In this report, we added 9 candidates between  $0.5 \cos \theta$  and  $0.5\pi$  distribution, and also 9 candidates between  $0.5\pi$  and  $0.5 \sin \theta$  distribution as shown in Fig.1.

All the elements in  $\mathbf{C}_v$  are real for any PDF candidates in Fig.1. However, we found that the (1,3) and the (3,1) elements of  $\mathbf{C}_v$  often becomes complex in the actual POLSAR images. Therefore, the  $\mathbf{C}_v$  estimation in this report is modified by adding the phase coefficient  $\vartheta$  into (1,3)-element of the matrix.

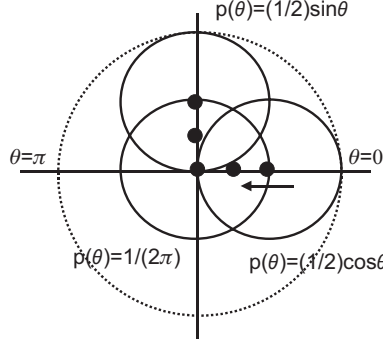


Figure 1: PDF of tree trunks and branches

### 3. Decomposition of Single and Double-bounce Components

When the most optimal  $\mathbf{C}_v$  is estimated by using ESPRIT method, we can remove the volume scattering ( $f_v \mathbf{C}_v$ ) and helix scattering components ( $f_c \mathbf{C}_c$ ) [2].

$$\tilde{\mathbf{C}} = \mathbf{C} - f_v \mathbf{C}_v - f_c \mathbf{C}_c = f_s \mathbf{C}_s + f_d \mathbf{C}_d = f_s \begin{bmatrix} |\beta|^2 & 0 & \beta \\ 0 & 0 & 0 \\ \beta^* & 0 & 1 \end{bmatrix} + f_d \begin{bmatrix} 1 & 0 & \alpha^* \\ 0 & 0 & 0 \\ \alpha & 0 & |\alpha|^2 \end{bmatrix} \quad (1)$$

where  $\mathbf{C}_s$  and  $\mathbf{C}_d$  denote covariance matrices corresponding to the single and double-bounce component.  $f_s, f_d$  are coefficients for each scattering contribution, and  $\alpha, \beta$  are complex unknowns for each scattering component. Estimation of the four unknowns ( $f_s, f_d, \alpha$ , and  $\beta$ ) is the next problem. Clearly the  $\tilde{\mathbf{C}}$  has a rank of 2. When we apply the eigen-decomposition to  $\tilde{\mathbf{C}}$ , it can be also expressed by

$$\tilde{\mathbf{C}} = [\mathbf{e}_1, \mathbf{e}_2] \begin{bmatrix} \lambda_1 & 0 \\ 0 & \lambda_2 \end{bmatrix} \begin{bmatrix} \mathbf{e}_1^H \\ \mathbf{e}_2^H \end{bmatrix} = \mathbf{E} \boldsymbol{\Lambda} \mathbf{E}^H = \mathbf{E} \boldsymbol{\Lambda}^{\frac{1}{2}} \mathbf{I} \boldsymbol{\Lambda}^{\frac{1}{2}} \mathbf{E}^H = \mathbf{E} \boldsymbol{\Lambda}^{\frac{1}{2}} \mathbf{U} (\mathbf{U}^H \boldsymbol{\Lambda}^{\frac{1}{2}} \mathbf{E})^H \quad (2)$$

where  ${}^H$  is complex conjugate.  $\mathbf{e}_i$  and  $\lambda_i (\lambda_1 \geq \lambda_2)$  are the eigenvector and corresponding eigenvalue of the  $i$ -th component. The third eigenvalue,  $\lambda_3$ , is zero, then we omit this component in (2). The matrix  $\mathbf{U}$  is an unitary matrix  $\mathbf{U}$  defined by

$$\mathbf{U} = \begin{bmatrix} e^{j\phi} \cos \theta_U & e^{j\delta} \sin \theta_U \\ -e^{-j\delta} \sin \theta_U & e^{-j\phi} \cos \theta_U \end{bmatrix} \quad (3)$$

When the volume and helix scattering component can be removed correctly,  $\lambda_1 \geq \lambda_2 > 0$  holds. It can be also used to check the validity of the removal processing.

Sum of the eigenvalues,  $\lambda_1 + \lambda_2$ , corresponds to sum of powers by the single and double bounce scattering components,  $P_s + P_d$ , where  $P_s = \lambda_1 \cos^2 \theta_U + \lambda_2 \sin^2 \theta_U$ . and  $P_d = \lambda_1 \sin^2 \theta_U + \lambda_2 \cos^2 \theta_U$ . The dominant component between the single and the double-bounce components can be estimated easily[2,3]. Without loss of generality, we assume the single-scattering component is dominant in the followings. With some algebraic calculations, we obtain the following inequality.

$$\frac{\lambda_2}{\lambda_1} \leq \frac{P_d}{P_s} = \frac{\lambda_1 \sin^2 \theta_U + \lambda_2 \cos^2 \theta_U}{\lambda_1 \cos^2 \theta_U + \lambda_2 \sin^2 \theta_U} = \frac{k^2 + \lambda_r}{1 + \lambda_r k^2} < 1 \quad (4)$$

$$0 \leq k = \frac{\sin \theta_U}{\cos \theta_U} = \tan \theta_U < 1, \quad \lambda_r = \frac{\lambda_2}{\lambda_1} \quad (5)$$

As shown here, when  $k$  can be determined, contribution of powers,  $P_s$  and  $P_d$  can be estimated uniquely. Using (2), (1) and (4), we can obtain following relation between  $\alpha, \beta$ , eigenvector and eigenvalues of  $\tilde{C}$

$$\beta = \frac{[\mathbf{e}_1]_1 - \sqrt{\lambda_r} [\mathbf{e}_2]_1 e^{-j\psi} k}{[\mathbf{e}_1]_3 - \sqrt{\lambda_r} [\mathbf{e}_2]_3 e^{-j\psi} k}, \quad \alpha = \frac{[\mathbf{e}_1]_3 + \sqrt{\lambda_r} [\mathbf{e}_2]_3 e^{-j\psi} k^{-1}}{[\mathbf{e}_1]_1 + \sqrt{\lambda_r} [\mathbf{e}_2]_1 e^{-j\psi} k^{-1}}, \quad \psi = \phi + \theta_U \quad (6)$$

Above equations shows that  $\alpha$  and  $\beta$  can be the function of  $k$  and  $\psi$ . Considering physical scattering process, we can impose following restrictions in Eq.(6) : 1)  $Re[\alpha] < 0 \& Re[\beta] > 0$ , 2)  $|\beta| < 1$ , and 3)  $|\alpha| < 1$

Possible values of  $k$  and  $\psi$  should be holds these restrictions. Therefore, we can limit range of  $k$ , and limit range of scattering power rate ( $P_d/P_s$ ). To determine  $P_s$  and  $P_d$ , we adopt mean value of possible  $ks$  in this method. As shown in this section, the most possible combination of decomposition in single and double bounce is searched by the proposed technique. Therefore more proper decomposition results than those by the conventional technique can be obtained by the proposed technique.

## 4. Experimental Results

Experimental data used in this study is the SIR-C/X-SAR data of the Tien Shan test site shown in Fig.2. The evaluated forest area is also marked in the figure.

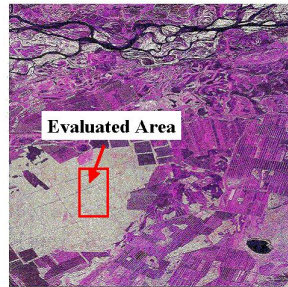


Figure 2: SIR-C/X-SAR Image of the Tien Shan test site

Table 1: Ratio of the number of area with a negative value in the evaluated area

	Proposed technique	Conventional technique
Single-bounce Scattering	0.37%	5.8%
Double-Bounce Scattering	0.70%	0.86%

Figures 3(a) and (b) shows the estimated  $P_s$  and  $P_d$ , respectively, by the proposed technique. Also, those by the conventional technique [2] are shown in Figs. 4(a) and (b). White area in these figure are the area where the estimated power becomes negative. Table.1 shows the ratio of the area having negative power. Clearly we can say that the number of area with a negative value decreases by the proposed technique compared with those by the conventional technique [2].

Figures 5 show selected PDF among the candidates shown in Fig.1 and histogram of the PDFs. Fig. 6(a) and (b) show the estimated phase of  $C_v$  discussed in Sect.2. As shown in Fig.5(a) and (b), almost all the estimated  $C_v$  have the PDF of  $\sin\theta$ -type distribution, which coincides the fact that the vertically distributed trunks and branches are dominant in this area. And as shown in Fig.6 (a) and (b), the estimated phase  $\vartheta$  is distributed around  $-21.6$  [deg.]( $-0.38$  [rad.]). This result shows that the off-diagonal elements ((1,3) and (3,1)) often become complex in the actual POLSAR data.

## 5. Conclusions

In this paper, we propose a modified scattering model decomposition technique for Pol-InSAR dataset. In the estimation of volume scattering component by the technique, we apply the ESPRIT-based Pol-InSAR technique used for forest height estimation of Pol-SAR data[4]. Also we consider more realistic assumptions for the decomposition of single and double-bounce scattering components.

Experimental results of the proposed technique and conventional technique [2] are provided. These results show that the proposed technique can suppress the problem of negative component occurrence more effectively than the conventional technique [2]. Therefore, it can be said that the stable scattering model decomposition can be realized by the proposed technique.

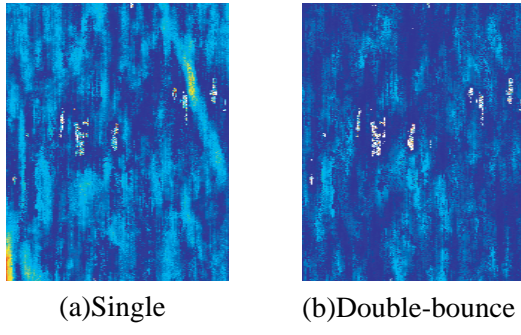


Figure 3: The proposed technique

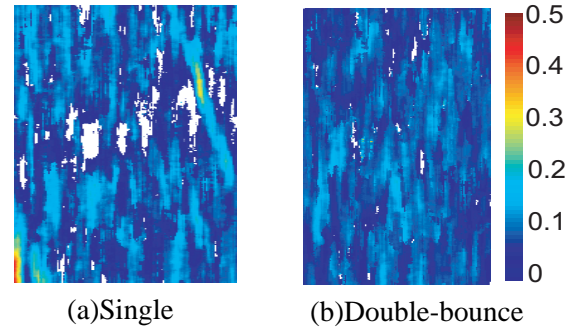


Figure 4: The conventional technique

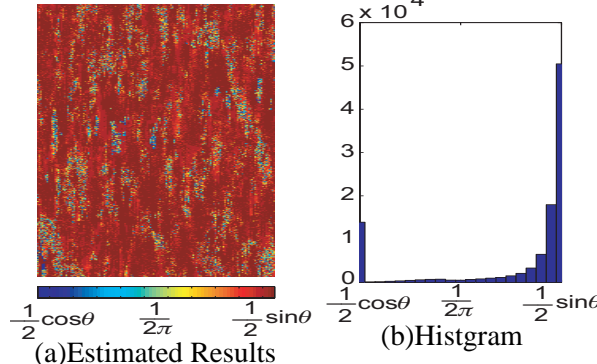


Figure 5: PDFs

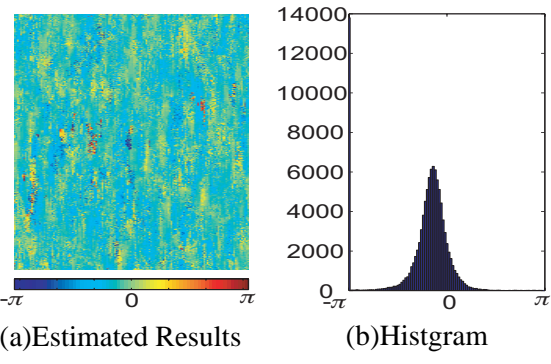


Figure 6: phase  $\vartheta$

## References

- [1] A.Freeman, S.L.Durden, "A three-component scattering model for polarimetric SAR data," IEEE T-GRS, vol.36, no.3, pp.936-973, May.1998.
- [2] Y.Yamaguchi, T.Moriyama, M.Ishido, H.Yamada, "Four-component scattering model for polarimetric SAR image decompositon," IEEE T-GRS, vol.43, no.8, PP.1699-1706, Aug, 2005.
- [3] H.Yamada, H.Okada, Y.Yamaguchi, "Accuracy Improvement of ESPRIT-based Polarimetric SAR Interferometry for Forest Height Estimation," Proc. of IEEE International Geosci. Remote Sens. Symposium 2005, July 2005.
- [4] H.Yamada, Y.Yamaguchi, Y.Kim, E.Rodriguez, W.M.Boerner, "Polarimetric SAR Interferometry for Forest Analysis Based on the ESPRIT Algorithm," IEICE Trans. Elect., vol.E84-C, No.12, pp.1917-1924, Dec.2001.
- [5] M.Yamazaki, H.Yamada, Y.Yamaguchi, "Accuracy improvement of forest height estimation with ESPRIT algorithm using four-component scattering-model decomposition," IEICE Technical Report, AP2005-138,pp.37-40,Jan.2006 (in Japanese).
- [6] H.Yamada, M.Yamazaki, Y.Yamaguchi, "On Scattering Model Decomposition of POLSAR Image and Its Application to the ESPRIT-Based Pol-InSAR," EUSAR2006, on CD-ROM, May 2006.